Review

A brief review of the ionic conductivity enhancement for selected oxide electrolytes

Shiqiang (Rob) Hui *, Justin Roller, Sing Yick, Xinge Zhang, Cyrille Decès-Petit,
Yongsong Xie, Radenka Maric, Dave Ghosh

NRC Institute for Fuel Cell Innovation, Vancouver, BC V6T 1W5, Canada

Abstract

The advantages of lowering the operation temperature of SOFCs have attracted great interest worldwide. One of the major barriers to decreasing the operation temperature is the ohmic loss of the electrolyte. Maximizing the electrolyte ionic conductivity is of significant importance, especially in the absence of new electrolyte materials. The ionic conductivity of electrolytes can be influenced by many parameters. There has been an enormous effort in the literature for the improvement of the electrolyte ionic conductivity. From a practical point of view, this paper reviews various approaches to enhancing the ionic conductivity of polycrystalline zirconia- and ceria-based oxide electrolytes in the light of composition, microstructure, and processing. Suggestions are given for future work.

Contents

1. Introduction

For reasons related to long-term stability and cost, decreasing the operation temperature of solid oxide fuel cells (SOFCs) down to 500–700 °C has attracted worldwide interest [1]. Decreased operation temperature, however, requires increased electrolyte ionic conductivity and enhanced electrode reaction activity. In the absence of available electrolyte materials at low tempera-tures, maximizing electrolyte ionic conductivity is of significant importance, as is the reduction of electrolyte thickness. Understanding the various factors that influence ionic conductivity can help to optimise conditions for further improvement of electrolyte properties.

Enormous amounts of effort can be found in the literature on ionic conductivity improvements for the oxide electrolyte materials, including zirconia-based oxides, ceria-based oxides, lanthanum gallate-based oxides, and bismuth-based oxides [2–6]. Zirconia-based electrolytes, such as yttria-stabilised-ZrO_2 (YSZ), are the most popular materials employed as the electrolyte in SOFCs because of its attractive ionic conductiv-

* Corresponding author. Tel.: +1 604 221 3111; fax: +1 604 221 3001.
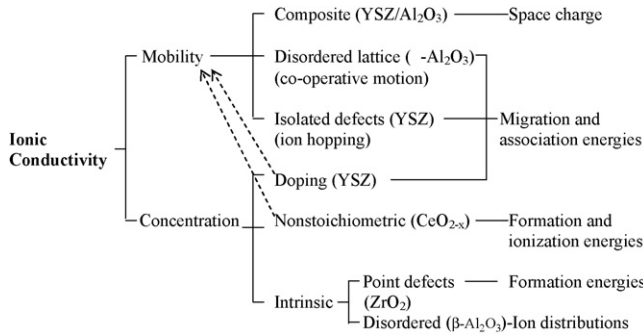*E-mail address:* rob.hui@nrc-cnrc.gc.ca (S. Hui).

Fig. 1. The major sources of ionic carriers in oxides and their respective mobilities compiled from literatures.
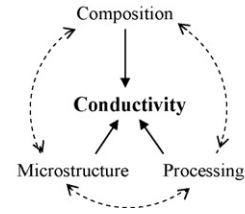

Fig. 2. The correlation of composition, microstructure, processing, and electrical conductivity in polycrystalline materials under given temperature and surrounding atmosphere.

ity, stability in both oxidising and reducing environments, and compatibility with the electrode materials [5,6]. However, at lower temperatures, the ionic conductivity of YSZ is much lower than that of ceria-based electrolytes such as gadolinia-doped ceria (GDC) or lanthanum gallate-based electrolytes such as $La_{0.8}Sr_{0.2}Ga_{0.8}Mg_{0.2}O_{3-\delta}$ (LSGM). Alternatively, ceria-based electrolytes have been considered for low-temperature applications, similar to the LSGM in terms of cost, processing, and stability. However, further enhancement of ionic conductivity and stability in reduction conditions is still required for ceria-based electrolytes.

The electrical conductivity (σ) can be expressed as $\sigma = nq\mu$, where n is the charge carrier concentration (cm^{-3}), q is the charge (in coulombs), and μ is the mobility of the charge carrier ($cm^2\,s^{-1}\,V^{-1}$). Thermodynamically and kinetically, the electrical conductivity in an oxide can be related to the temperature, oxygen partial pressure in the surrounding gas atmosphere, the type and concentration of dopants, and the microstructure [7,8]. The major sources of ionic carriers in oxides and their respective mobilities are summarized in Fig. 1, in which the broken arrows indicate where large numbers of carriers generated via deviation from stoichiometry or doping may alter the carrier mobilities [7,8]. For oxygen ion transport in zirconia- and ceria-based electrolytes the charge carriers are oxygen vacancies. The following equation is usually applied to oxygen ionic conductors:

$$\sigma T = A \exp\left(\frac{-E_a}{kT}\right) \tag{1}$$

where σ is the ionic conductivity, T the absolute temperature, A pre-exponential constant, and E_a is the activation energy. The activation energy normally includes energy terms for formation and migration of oxygen vacancies. In the extrinsic regime, the activation energy is dominated by the migration energy. In this case, the activation energy can be represented by the migration energy for the doped oxide ionic conductors in the extrinsic regime. The point defects without association were considered in the discussion above. If oxygen vacancies form defect association within the oxide, the dissociation energy to break this complex at high temperature also has to be considered in the activation energy.

The effects of various factors, such as grain boundary, local structure, microdomain, grain size, composition, dopants, impurity, and processing on ionic conductivity in zirconia-

and ceria-based electrolytes have been discussed elsewhere [5,6,9–11]. In this work, the effects in terms of composition, microstructure, and processing on the electrical conductivity for polycrystalline zirconia- and ceria-based electrolytes are reviewed. As shown in the following discussion, these parameters are correlated to each other. Composition, dopant concentration, and processing conditions can change the properties of grains and grain boundaries. This, in turn, affects the effectiveness of the dopants. Grain boundary properties can also vary by grain size. Composition, microstructure, and processing are fully related to each other in electrical properties. These relations with electrical conductivity are illustrated in Fig. 2.

2. Enhancement from composition

The isothermal conductivity of rare earth-doped ceria and zirconia has been particularly well studied in the literature. The ionic conductivity of electrolytes can be maximized through composition modification by selecting an appropriate aliovalent dopant and its optimal concentration [5,6,9–11]. The doping can be either homogeneous to form a solid solution or heterogeneous to form a composite. For homogeneous doping, adding aliovalent cations to the zirconia or ceria produces oxygen vacancies, which provide the pathway for the conducting oxygen ions. The existence and the contribution of microdomains to the ionic conductivity may suggest that the oxygen vacancies are not simple random distributions. A solid solution region where the parent cubic fluorite structures of zirconia and ceria is preserved generally defines the composition range.

In the case of zirconia-based systems, Sc^{3+} is the most effective dopant among Ca^{2+}, Y^{3+}, Sm^{3+}, etc., whereas Mg^{2+} is the least efficient in providing an open pathway for conduction [12]. However, the initial high conductivity in ScSZ is followed by at first a rapid and then a gradual drop in conductivity. This behaviour of the conductivity degradation has been attributed to the existence of a metastable t'-phase, as discussed in the following section on the effect of grain boundaries. Regarding doped ceria, highest conductivities have been reported for either Sm- or Gd-doped ceria. It is generally recognized that the most effective aliovalent addition appears to be defined by the relationship between the ionic radii of the additive and the parent lattice [9,13,14]. However, there is still discrepancy in understanding the relationship between the dopant properties and the ionic conductivity. Kilner has suggested that a better means of evaluating the relative ion mismatch of dopant and host would

be to compare the cubic lattice parameter of the host oxide and the pseudocubic lattice parameter of the corresponding dopant oxide. In this way, it is explained why Gd and Sc are excellent dopants in ceria and zirconia, respectively [15]. Kim proposed the concept of a critical ionic radius for the dopant, which is an ideal dopant cation radius that would give the same lattice constant as that of the undoped electrolyte [16]. The critical ionic radius for a trivalent dopant in ceria is 1.038 Å. However, although Gd- or Sm-doped ceria have higher ionic conductivity than Y-doped ceria, the best match for either the ionic radius of Ce^{4+} (0.97 Å) [17] or the critical ionic radius in ceria is Y^{3+} (1.019 Å) rather than Gd^{3+} (1.053 Å) or Sm^{3+} (1.079 Å). Kilner et al. and Catlow explained that a smaller ionic size mismatch between the host and a dopant was preferable for obtaining a high conductivity [18,19].

In addition to the single doping in zirconia and ceria, multiple doping appears to improve the electrolyte ionic conductivity further. Several ternary systems involving yttria-stabilised zirconia have been studied from the viewpoint of structure and electrical properties with the third component being calcia, scandia, rare-earth oxide, or magnesia [20–31]. Depending on chemical and phase composition, these generally have improved ionic conductivities, although in some cases deterioration of the ionic conductivity has been observed. Mucko has studied the electrical conductivity for a series of YSZ systems with the addition of calcia at 350 °C [20]. They found that the ionic conductivity of YSZ with a small amount of calcia added could be enhanced about three times higher compared to that of YSZ without calcia. This effect on the ionic conductivity was attributed to local microstructure [20]. Gong et al. also observed an ionic conductivity improvement for zirconia doped with 6 mol% calcia and 4 mol% yttria at temperatures above 830 °C [21]. They concluded that such improvement might be due to the increase in the concentration of oxygen vacancies linked to the low activation energy. Kaneko et al. examined the electrical conductivity of zirconia co-stabilised with 8 mol% scandia and yttria by impedance measurements [22]. The electrical conductivity increased at temperatures above 370 °C and decreased below this temperature when scandia-doping levels were increased. Souza and Chinelatto have studied the effect of rare earth additions on the electrical conductivity of impure zirconia doped with 12 wt.% yttria [23]. The additions of rare earth led to an electrical conductivity close or higher than that of electrolytes prepared from high-purity zirconia. SEM examination of the grain boundaries indicated enhanced impurity segregation [23]. Souza and Chinelatto suggested that the conductivity improvement was most likely due to the increased segregation of impurities on grain boundaries rather than the effect of dopant properties [23]. However, elastic driving forces in YSZ can be significant for segregation phenomena when a large size mismatch exists between dopant and host cations, as reported by Kilner [24]. The elastic field generated by the size mismatch of dopants with the YSZ matrix might further enhance the segregation of the small radius impurity ions. The segregation enthalpy can be explained by an interface contribution, a contribution due to solute–solvent interaction, an elastic strain energy contribution, and an electrostatic term [25]. Lee and his colleagues studied the electrical conduc-

tivity and phase stability of ZrO_2 co-doped with Sc_2O_3 and CeO_2 [26]. They claimed that such electrolyte systems showed much higher electrical conductivity than YSZ in the temperature range of 300–1100 °C and better long-term stability than any other Sc–ZrO2-based electrolyte. In addition, the phase of the Sc_2O_3 and CeO_2 co-doped ZrO_2 was stable (as a cubic phase) up to 1550 °C. Shiratori et al. added magnesia to YSZ in order to better match the coefficient of thermal expansion (CTE) with other components without significant degradation in ionic conductivity [27]. It was found that when the molar fraction of magnesia was less than 0.6, the conductivities of the composites were in the same range as the conductivity of pure 3YSZ at temperatures of 700–900 °C.

The effects of multiple doping on the conductivity of ceria-based electrolytes have also been reported. Ralph et al. have studied the effect of oxide additions on the total and grain boundary conductivity for Gd-doped ceria with compositions of $Ce_{1-x-y}Gd_xM_yO_2$ (M = Ca, Fe, Pr; x = 0.09, 0.10, 0.18, 0.19, 0.20; y = 0.01, 0.02) [28,29]. Small amounts of oxide additions have significantly enhanced the grain boundary conductivity compared to that of Gd-doped ceria without additions. Maricle et al. have studied similar electrolyte systems with the composition of $Ce_{0.8}Gd_{0.19}M_{0.01}O_2$ (M = Pr, Sm) [30] and demonstrated that these oxide additions also extended the lower oxygen partial pressure limit of the electrolyte domain boundary by two orders of magnitude. However, Ralph et al. did not confirm the effect of second phase additives on the width of electrolyte domain for the same electrolyte composition.

Mori et al. have proposed a concept of an effective index from the crystallographic point of view to maximize the ionic conductivity in ceria-based systems [31,32]. The effective index is defined as $(avg.r_c/eff.r_o) \times (r_d/r_h)$, where $avg.r_c$ is the average ionic radius of the cations, $eff.r_o$ the effective oxygen ion radius, r_d the average ionic radius of the dopant, and r_h is the ionic radius of the host element (Ce^{4+}). The relationship between effective index and conductivity for ceria with different dopants is shown in Fig. 3. They found that the electrolyte materials have not only
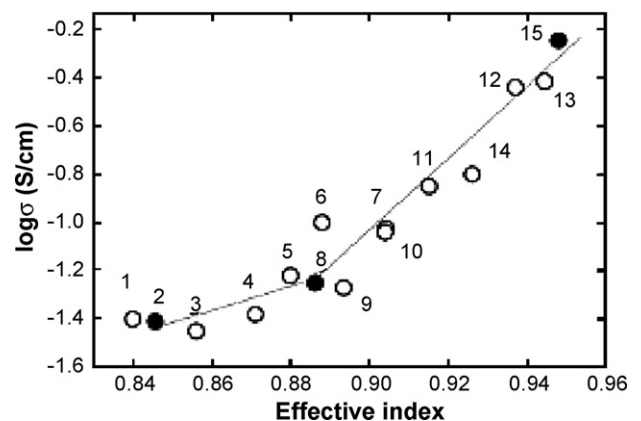
Fig. 3. Relationship between effective index and conductivity at 800 °C: (1) CSO20, (2) CSO21, (3) CSO25, (4) CSO50, (5) C(SCa50)O20, (6) C(SCa50)O22.5, (7) C(SCa50)O25, (8) C(SSr20Ba5)O17.5, (9) CLO12.5, (10) CLO15, (11) CLO17.5, (12) C(LSr10)O17.5, (13) C(LSr20)O17.5, (14) C(LSr20Ba3)O17.5, (15) C(LSr20Ba5)O17.5, where C is for Ce, S for Sm, and L for La from Mori et al. [31].

improved the ionic conductivity but also the increased resistance of ceria reduction from Ce^{4+} to Ce^{3+} in reducing atmospheres. Analysis of HRTEM revealed that an electrolyte with single doping had large microdomains (over 10 nm), while one with multiple doping could reduce the microdomain to be around 1–3 nm, suggesting that small microdomains could benefit the oxygen ion transportation through the lattice. However, the stability of the small microdomain against the annealing of the electrolyte was not reported [31,32].

An alternative route to enhancing the ionic conductivity by composition is to employ heterogeneous dopants that are insoluble or soluble with low limit in the zirconia or ceria bulk structure. Alumina has been most commonly used for such purpose in YSZ due to its limited solubility. Depending on the alumina concentration and electrolyte materials, the additions were either beneficial or detrimental to the electrical conductivity. TEM and microanalytical characterization revealed that the addition of alumina to zirconia, at levels beyond the solubility limit, results in an improvement due to grain boundary interactions between second-phase alumina particles and the silicate films [33]. EDX microanalysis using a finely focused electron probe showed that the small inclusions of dark contrast within the alumina were rich in silicon. The silicate phases exist as impurities in the electrolyte and can cause a significant blocking to grain boundary conductance, as discussed in the next section. Drennan et al. observed that there was a strong interaction between the boundaries and the alumina that took the form of boundary pinning, i.e. glassy pocket formations at the interface [34]. Butler et al. suggested that the grain boundary conductivity improvement only occurs at alumina levels sufficient to establish local grain boundary thermodynamic equilibrium and eliminate silica-rich liquid phases in favour of mullite or mullite in local equilibrium with the free alumina [35,36]. Steele and Butler reported that there is a smaller improvement in overall conductivity when additions of alumina are made in YSZ of higher purity [37]. AC impedance measurements demonstrated that the effect was essentially related to improvements in the bulk conductivity due to Al^{3+} doping, and the improvement depended on the silicate level in the YSZ. However, Guo et al. reported that the addition of alumina in the amounts of 0.4 mol% increased both grain and grain boundary resistivities [38]. The grain resistivity was increased by only 3%, whereas the grain boundary resistivity was increased by 600%. Miyayama et al. reported an alumina solubility limit of 0.6 mol% in YSZ [39]. They found grain and grain boundary conductivities decreased and grain growth was promoted below the solubility limit. However, the grain boundary conductivity increased and grain growth was inhibited above the solubility limit of alumina. Feighery and Irvine [40] also investigated the effect of alumina additions on the electrical conductivity of 8 mol% YSZ. They reported that approximately 1 wt.% alumina dissolves into the structure of YSZ when sintered at 1500 °C for 24 h. The high-temperature conductivity increases for 1 wt.% alumina and then decreases to approximately the same conductivity as the undoped 8YSZ. The conductivity remained constant until 10 wt.% alumina and subsequently decreased rapidly with further addition of alumina. Badwal and Drennan found that

scandia-stabilised zirconia (ScSZ) could also benefit from the addition of alumina [41].

The addition of alumina to ceria-based electrolytes has also been studied. Zhang et al. examined the effect of alumina addition to 20% Gd doped ceria and found in the 0–10% alumina range the overall conductivity was lower [42]. This was due to a slight increase in grain interior conductivity and a rapid decrease in grain boundary conductivity that can be observed with increasing alumina content. This is in contrast to previous findings that alumina doping in YSZ leads to a slight decrease in grain interior conductivity, but a remarkable improvement in grain boundary conductivity. Increased grain interior conductivity for alumina-doped 20% GDC was postulated to be largely attributed to the solid state reaction between alumina and gadolinia, which results in a decrease in the amount of gadolinia dissolved in ceria.

There has also been an effort to make ceria-zirconia composite electrolytes to either improve the ionic conductivity or take advantage of both components in terms of stability and conductivity. The ceria-zirconia composite electrolytes were either doped ceria particles embedded in a continuous YSZ matrix [43] or YSZ/doped ceria multi-layers [44,45]. In both cases, the highly conductive-doped ceria reduced the effective thickness of the relatively low-conductivity YSZ layer while the continuous YSZ layer served as a barrier to electronic conduction through the doped ceria. Luo et al. have prepared GDC–YSZ composites from powders and sintered them over a temperature range from 1400 to 1600 °C [46]. They found that the ionic conductivity of the electrolyte decreased with the 10–50 wt.% addition of GDC to YSZ. XRD examination of the composites revealed the formation of a solid solution that led to the reduced conductivity. Horita et al. examined films using a thin layer of YSZ sandwiched between two layers of GDC and found poor electrical conductivity, compared with theoretical values, due to the formation of a solid solution phase [47]. The solid solution phase likely reduced the ionic conductivity of the GDC–YSZ–GDC composite and raised the activation energy for ionic conduction. In addition, pores have been formed at the interface of the GDC–YSZ layers and this could have contributed to reduction of conductivity. The conductivities of composite electrolytes of YSZ–$CGO_{0.5}YSZ_{0.5}$–CGO were an order of magnitude lower than either YSZ or CGO [48]. Again, pores were found between the layers. The effect of SDC particle size (diameter 1–840 μm) on the stability of YSZ–SDC composite electrolyte and the influence of YSZ–SDC solid solution on SOFC performance have both been studied. Mishima et al. found that the temperature for YSZ–SDC reaction decreased with decreasing SDC particle size. Zhou et al. also studied the interaction between GDC and YSZ through XRD analysis [49]. The change of phase for GDC and YSZ powders sintered at different temperatures indicated that the interaction started around 1200 °C. Most recently, Price et al. reported that the formation of YSZ–SDC solid solution in the nanocrystalline system was as low as 900 °C [50]. Mishima et al. found that the OCV of the cell significantly decreased with the formation of YSZ–SDC solid solution [43]. It was believed that the poor ionic conductivity of the zirconia–ceria solid solution attributed the deterioration of the cell perfor-
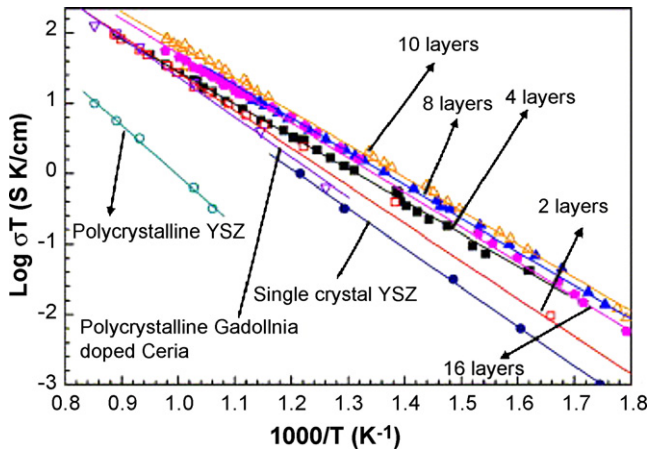
Fig. 4. The dependence of the ion conductivity on the number of layers with a constant total film thickness [53].

Fig. 5. Illustration of a typical impedance plot for a polycrystalline sample with equivalent circuits.

mance. Kimpton et al. revealed that electrical conductivities of both $Zr_{0.75}Ce_{0.08}Sm_{0.17}O_{1.915}$ and $Zr_{0.75}Ce_{0.08}Y_{0.17}O_{1.915}$ were significantly lower than that of the YSZ at 800 °C. Excessive distortion of the oxygen ion conduction path by large size ionic dopants was found to be responsible for the decline in conductivity [51]. Studies from Zhou et al. [49] and Zhu [52] on the solid solution revealed that it was a mixed electronic and ionic conductor. An n-type electronic conducting behaviour was observed in the oxygen partial pressure of $1–10^{-18}$ atm at 800 °C. The solid solution had a lower conductivity and larger expansion during reduction than that of GDC or YSZ as well [49]. However, when the thickness of the ZrO_2–CeO_2 film was down to the nanometer level, the electrical behaviour may change correspondingly. Azad et al. have systematically investigated the nanosize effect on oxygen ionic conductivity of gadolinia-doped multi-layer ZrO_2–CeO_2 films [53]. It was observed that oxygen ionic conductivity increased as a function of the number of film layers while keeping the total thickness constant. The increases were higher than either single crystal YSZ thin films or polycrystalline YSZ and Gd_2O_3 doped CeO_2, as shown in Fig. 4.

3. Enhancement from microstructure

3.1. Effects of grain boundaries

The electrical conductivities of polycrystalline materials are greatly influenced by their microstructures, i.e. the properties of grain and grain boundary. Grain boundaries are the crystallographic mismatch zones whose properties are determined by mismatch of the lattices, impurities (or second phase segregation), space charge, microcracks, or a combination of all of these. In many polycrystalline materials grain boundaries provide a region of relatively rapid mass transport compared to the bulk properties of the crystallites. However, in zirconia- or ceria-based electrolytes the grain boundaries have a lower effective charge carrier concentration and thus result in a highly resistive grain boundary phase. AC impedance spectroscopy is widely employed to obtain information related to the electrical behaviour of both the bulk (grain interiors) and the grain
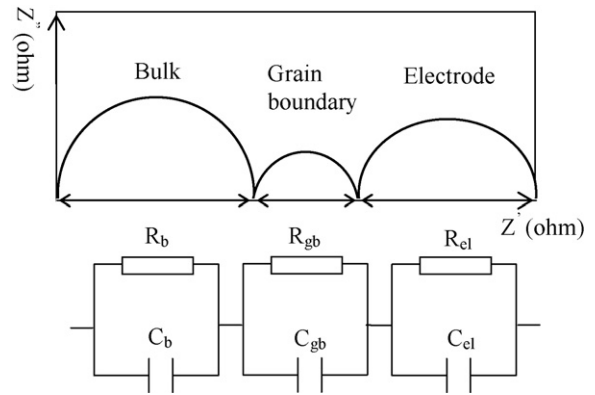
boundaries. A typical impedance plot for a polycrystalline sample with equivalent circuit is illustrated in Fig. 5. For a sample with a length of L and cross-section area of A, the bulk conductivity, σ_b, σ, and the total grain boundary conductivity, σ_{gb}, can be expressed as $\sigma_b = L/AR_b$ and $\sigma_{gb} = L/AR_{gb}$, where R_b and R_{gb} are the bulk and grain boundary resistance, respectively. Then, the total electrical conductivity, σ^T, can be calculated from equation $1/\sigma^T = 1/\sigma_b + 1/\sigma_{gb}$ [54]. Assuming that all the grains are cubic with equal size of d_g, the grain size is much smaller than grain boundary thickness, δ_{gb}, and that the contribution to the conductivity parallel to the grain boundaries is negligible, the specific grain boundary conductivity can be estimated by the following equation [55].

$$\sigma_{gb}^{sp} = \frac{\sigma_{gb}^T \delta_{gb}}{d_g} \tag{1}$$

Assuming reasonable values for the grain boundary thickness, order of magnitude estimates of specific grain boundary conductivity have been reported [56]. Impedance studies on both microstructured and nanostructured YSZ showed that the electrical conductivity in grain boundaries is 2–3 orders of magnitude smaller than in the crystallite volume. Correspondingly, the activation energy of the electrical conduction at interfaces with values in the range of 1.0–1.2 eV is significantly higher than the values of 0.84–0.93 eV observed for the bulk conductivity [56,57]. A brick-layer model has been employed to correlate the microstructure with the grain and grain boundary conductivity and to explain the variation of ionic and electronic conductivity in electrolytes as a function of grain size [58–60]. In this model, it is assumed that the ceramic samples consist of grains with a high conductivity, separated by relatively thin, uniform grain boundaries. For a positive space–charge potential, positive carriers, such as oxygen vacancies and electron holes, are depleted and negative carriers, such as electrons, are enhanced in grain boundaries. The relative depletion of oxygen vacancies is equal to the square of the relative enhancement of electrons, leading to increased n-type conductivity. Positive space-charge potentials of 0.3 and 0.25 V have been obtained for polycrystalline ceria and YSZ, respectively [61,62]. Guo and Maier reported that the magnitude of ∼0.3 V for ceria is sufficient to cause enhancement of the n-type conductivity of an order of magnitude. As

a consequence, a transition from predominantly ionic to electronic conductivity could occur at a grain size of about 60 nm in ceria [62].

It has been widely reported that impurities such as silica greatly decrease the grain-boundary conductivity in zirconia and ceria [57,61,63–66]. Badwal and Rajendran found that the addition of only 0.2 wt.% silica was sufficient to decrease the grain-boundary conductivity of YSZ by a factor greater than 15 [65]. Therefore, eliminating the effect of impurities on the grain boundary can benefit the ionic conductivity of the electrolyte. A number of strategies have been suggested to control the silica-rich grain boundary, including specialized heat treatments, the application of pressure, and various additives [57,61,63–66]. Varying grain size at concentrations low enough that a discrete siliceous film does not form can systematically vary the boundary coverage of silicon. Experimental studies on fully dense, highly pure specimens of nano and microcrystalline calcia-doped or yttria-doped zirconia showed a significant increase of the conductivity at interfaces with decreasing crystallite size down to nanometer size [57,67]. Ralph et al. reported that ionic conductivity could be enhanced by trapping impurities by forming low-temperature compounds with small amount of second phase additives [68]. Some oxides can form eutectic compounds with impurities in grain boundary. These compounds may have eutectic temperatures below the electrolyte sintering temperatures, which can be trapped to certain areas in the grain boundary upon cooling.

However, the grain boundary conductivity remains lower than the bulk value, even for highly pure electrolyte materials where the grain boundary has no significant amount of silica covering [56]. Therefore, the grain boundary blocking in YSZ is also ascribed to an intrinsic property due to the formation of electric space charge layers at grain boundaries, which was supported by the segregation behaviour of dopant cations [69,70]. The strain and electrostatic energies of the electrolyte could be reduced through segregation of charged species, such as impurities and/or defects in the grain boundaries, leading to a positive or negative potential. Guo et al. have revealed the existence of positive space charge potentials in polycrystalline yttria-doped zirconia and ceria [61,62]. Therefore, positively charged ionic defects will be depleted while those with opposite charge will be accumulated in the space charge region in zirconia- or ceria-based electrolytes. Electrochemical and theoretical studies by Guo and Maier [61] on microcrystalline zirconia doped with 2–8 mol% yttria indicated the presence of an ~5-nm wide, poor conduction layer at interfaces. Both analytic studies by means of high-resolution transmission electron microscopy (HRTEM), electron energy loss spectroscopy (EELS), and atomistic modeling showed a significant segregation of Y^{3+} depleted zones, a negative space charge, and a very low concentration of oxygen vacancies prevail on the length scale corresponding to the Debye length of a few nanometers [61,67,71,72].

The blocking grain boundary effects can also be significantly affected by either temperature or dopant level or type [73–75]. When the temperature is high enough, the grain boundary resistance appears to become negligible in comparison to the grain resistance. This temperature varies with dopant types

and concentrations in zirconia or ceria. Nowick et al. observed that the grain boundary effect becomes negligible above a dopant concentration of 15 mol% regardless of the dopant type in ceria [73,74]. Therefore, the impact of grain boundary on the ionic conductivity of electrolyte is especially important for lower-temperature applications. Hon et al. also found that the grain boundary contribution to the resistivity in ceria generally decrease with increasing dopant levels. They found that the temperature above which the grain boundary effect appears to become negligible for ceria doped with 9 mol% Gd_2O_3, Sm_2O_3, or La_2O_3 are 725, 775, and 650 °C, respectively [75]. The blocking and unblocking grain boundary effects also depend on the homogeneous or heterogeneous materials. The formation of vacancies and excess electrons are easier in homogeneous media such as ceria [63,76]. Most recently, Kosacki et al. have investigated the effect of film thickness on the ionic conductivity for YSZ films [77]. They discovered that the ionic conductivity increases with decreasing thickness of YSZ film, as shown in Fig. 6. Similar results were reported for the ZrO_2–CeO_2 composite thin film [53]. These studies on the super-lattice and super-thin thin films (below 60 nm) at Oak Ridge National Laboratory and Pacific Northwest National Laboratory show that conductivity can be increased by an increase in the volume of unblocking interfacial/surface areas. As an example of the important role of unblocking grain boundary effects, the engineering of the unblocking grain boundaries can be a key to increasing the ionic conductivity in the future.

Many researchers have demonstrated the effect of different microdomains, or local lattice structures from different dopants, on the ionic conductivity as well. For instance, enhanced ionic conductivity in ScSZ has been attributed to the existence of a metastable tetragonal phase known as the t'-phase [78,79]. The formation of the t'-phase in yttria-stabilised zirconia requires
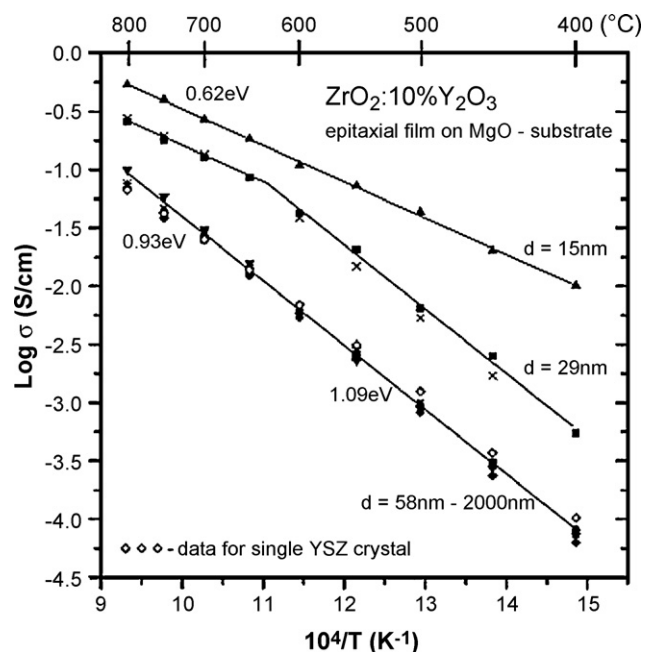

Fig. 6. Temperature dependence of the electrical conductivity determined for epitaxial YSZ thin films with different thicknesses [77].

very fast quenching from the melt, while the t'-phase can be easily formed in ScSZ in the cubic phase field and quenched by simply removing the sample from the furnace. This phase has a characteristic microstructure described as banding. These bands occur as the phase changes from cubic to tetragonal and the resulting strain is accommodated by the formation of twin bands. This banding rapidly disappears if the sample is annealed and the usual mottled grain structure develops, resulting in degradation of ionic conductivity [80]. The t'-phase contains high-dopant concentration, but is obviously in a metastable state at the normal operating temperature for SOFC applications. Yoshida et al. have investigated the local structures of doped ceria by extending X-ray absorption fine structure (EXAFS) measurements, showing that the ionic conductivity is remarkably affected by the local structures of dopant and Ce^{4+} ions [14]. The high ionic conductivity of LSGM has also been attributed to microstructural features such as internal interface structures [81,82]. O'Hayre et al. claimed that the ion conductivity in yttria stabilised zirconia and doped ceria could be enhanced by creating additional dislocation through conventional irradiation techniques [83]. Ion and/or electron irradiation causes the growth of vacancy clusters within the thin film and collapsing into Frank dislocation loops that exhibit high ion conductivity. Maximum ion conductivity is accomplished by spatially reorienting the Frank dislocation loops during a following heat-treatment of the membrane. Thus, the dislocation loops form surface-to-surface continuous dislocations allow ions to propagate between membrane surfaces with minimal activation energies. Further understanding of the formation and properties of microdomain with respect to conductivity may provide valuable insight into the design or improvement of oxygen ion conductors. Most recently, Guo and Waser have published a comprehensive review article for the electrical properties of the grain boundaries of oxygen ion conductors [84]. Various factors influencing the grain boundary electrical properties were reported from experimental and theoretical points of view.

The ionic conductivity in the zirconia- or ceria-based electrolytes can be further improved by introducing a liquid phase either in the grain boundaries or by forming composite electrolytes. Most recently, Fu et al. have examined the electrical conductivity of ceria chloride composite electrolytes containing GDC–LiCl–SrCl$_2$ [85]. The hot pressed composite showed superionic conductivity 2–10 times higher than GDC itself in the temperature range of 400–600 °C with reduced electronic conduction.

3.2. Effects of grain size

In recent years, there has been growing interest in exploring whether reducing the grain size down to the nanoscale in electrolytes can further enhance the ionic conductivity [56,76,86,87]. Nanocrystallinity introduces such a high density in the interfaces that the conduction properties may become interface-controlled. Many researchers have investigated the grain size dependence of conductivity in polycrystalline solid electrolytes and agreed that grain size effects could be observed when the grain size is below 100 nm. For nanocrystalline zirconia-based materials, Tien reported an increased electrical conductivity with decreased grain size for $Zr_{0.84}Ca_{0.16}O_{1.84}$ at temperatures below 800 °C [88]. The specimen of smaller grain size exhibited higher activation energy for grain boundary conduction. This value was found to be about 0.96 eV, whereas the activation energy for the specimen with large grain size lies in the range of 1.24–1.30 eV. Anderson's group has studied a series of nanostructured thin film materials spin-coated on an alumina substrate, including YSZ and ceria-based electrolytes [49,89]. The studies of Kosacki et al. on thin films of 16 mol% YSZ reported a remarkably enhanced conductivity and a lower activation enthalpy in nanocrystalline films (with average grain size of 20 nm) than in coarse-grained polycrystals [89]. Nanocrystalline YSZ exhibits an increase of about 2–3 orders of magnitude in electrical conductivity as compared to microcrystalline specimen. Activation energy is 1.23 and 0.93 eV for micro and nanocrystalline specimens, respectively, which is close to calcia-doped zirconia investigated by Tien [88].

For the nanocrystalline ceria-based electrolytes, Tschope and Birringer have compiled the experimental results on the electrical conductivity and their activation energy as a function of grain size [90]. The results showed that nanocrystalline ceria possesses an increased electrical conductivity and decreased activation energy when decreasing grain size. The quoted authors by Tschope and Birringer also concluded that nanocrystalline cerium oxide was found to be electronically conductive while microcrystalline cerium oxides exhibited predominantly ionic conductivity under the same temperature, oxygen partial pressure, and doping level [89]. Chiang et al. at MIT have ascribed the enhancement of electronic conductivity in nanocrystalline ceria to the decrease of defect formation energy at grain boundaries [91]. Maric et al. also studied nanostructured ceria and doped ceria with grain size ranging from 150 to 500 nm [92]. The powders of ceria and doped ceria were synthesized with an average particle size below 20 nm from a flame combustion method. Specimens with 99% theoretical density could be obtained by sintering pressed nanopowders at temperature as low as 1150 °C. In addition, the total electrical conductivities were also higher than that reported in the literature—a factor of four times higher at 500 °C.

However, the effect of grain size on the electrical conductivity in zirconia-based or ceria-based electrolytes may be not proportional monotonously in the whole range of grain size. Ioffe et al. have prepared 5.7 mol% YSZ specimens by hot-pressing at 1200 °C and investigated the effect of grain size between ~0.2 and ~18 μm on the conductivity of YSZ polycrystalline materials [93]. Dijk and Burggraaf investigated the effect of grain size between 0.4 and 20 μm on the ionic conductivity of $Gd_xZr_{(1-x)}O_{(2-0.5x)}$ [58]. Verkerk et al. explored the effect of grain size on grain boundary conductivity of YSZ [94]. Badwal et al. and Chen et al. also investigated the variation of electrical conductivity of YSZ as a function of grain size [95,96]. All of the authors above have observed a decrease in conductivity with decrease grain size in the range of 0.2–20 μm. Under this category, impedance measurements generally revealed a constant or slightly increased bulk conductivity and a decreased total grain

boundary conductivity associated with the decrease in grain size [55,89].

The variations in the electrical properties can be the results of many factors such as band structure modification due to spatial modulation of the lattice, quantum confinement of charge carriers, and dominant contributions from largely defective and strained grain boundaries in nanostructured materials [97,98]. More direct measurements of electronic and ionic conductivity for nanocrystalline electrolytes are required for further understanding the grain size effects.

4. Enhancement from processing

Processing conditions are another area that can greatly influence the electrical conductivity of electrolytes. These include different sintering processes in order to prepare ceramics with a controlled microstructure (grain size, density, purity). So, consequently the electrolyte composition and microstructure are fully related to sintering conditions. The influence of processing on the ionic conductivity of the electrolyte can help optimize the sintering conditions and further improve the electrical properties of the electrolyte. Different sintering conditions will result in diverse characteristics in the microstructures of the electrolyte such as grain size, grain boundary phases, and phase segregation on the boundaries, agglomeration, and relative density. The ionic conductivity varies strongly with the sintering conditions of the electrolyte [92,99]. Kleitz et al. [100] and Dessemond et al. [101] observed the high values of grain boundary resistance at sintering temperatures below 1300 °C due to the low relative density of the electrolyte. Gibson also observed the linear correlation between grain boundary conductivity and porosity [102]. A microstructure with full density is therefore an essential prerequisite for a high-performance ionic conductor.

The processing methods also have an effect on conductivity through the grain boundary. Shelmilt et al. have prepared dry-pressed and compression-molded pellets of Samaria-doped ceria (SDC) with identical powder [103]. The grain boundary activation energy was higher for compression-molded samples than for dry-pressed samples with 98% theoretical density. The different levels of impurities from two different routes might have led to the observed results. Therefore, the optimized processing should have less additives and steps to avoid the possible introduction of impurities into the electrolyte grain boundary. Aoki et al. reported that quenched calcia-doped zirconia exhibited higher boundary conductivity than the same sample after slow cooling [55], most likely due to the microdomain effect as mentioned in the previous section. Hirano et al. investigated the conductivity of 3–7 mol% ScSZ sintered at 1300 °C followed by a hot isostatic pressing [104]. They found a significant improvement in both the fracture strength and the electrical conductivity. Most recently, Mori et al. reported the influence of particle morphology from starting materials on the formation of microdomain and electrical conductivity in SDC [105]. They found that the electrical conductivity of sintered SDC prepared with different starting morphologies was different. The conductivity of materials prepared from spherical particles was much higher than that with elongated particles. The studies of HRTEM revealed
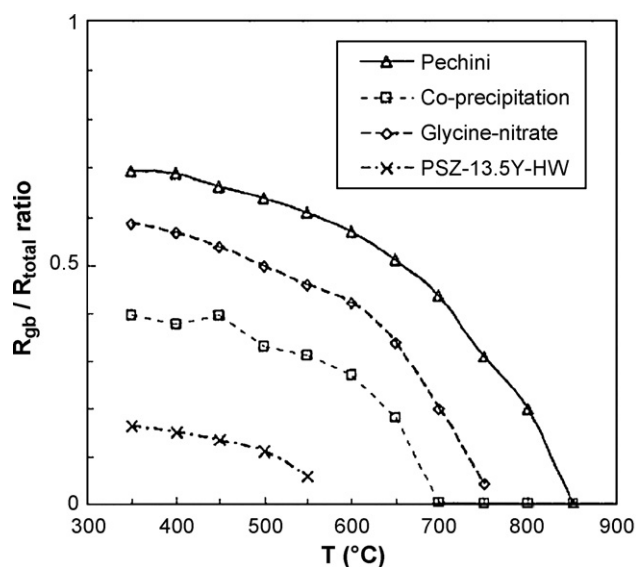

Fig. 7. The ratios of grain boundary/total resistivity as a function of temperature for 8YSZ [106].

that the size of microdomain was smaller for the samples made from round shape particles. Yamahara et al. have reported similar results for the YSZ prepared from different routes, as shown in Fig. 7 [106]. The total conductivity could be increased by as much as 50% when increasing sintering temperature or reducing powder particle size of polycrystalline 8YSZ.

5. Conclusions

Optimising the electrolyte composition, microstructure, and processing conditions can achieve maximum ionic conductivity. The following methods have been reported and reviewed for the enhancement of electrical conductivity. In the absence of available electrolyte materials at low temperatures, modification of grain boundary conditions and engineering of the electrolyte thickness in the nanoscale seem a most effective way to enhance the ionic conductivity of electrolytes.

(a) Doping of an alivalent cation into zirconia or ceria is an effective approach to improving the ionic conductivity.
(b) Multiple doping has been demonstrated to further enhance the ionic conductivity and chemical stability.
(c) Introducing a second phase to form a composite electrolyte may change the grain boundary condition and therefore vary the electrical conductivity of the electrolytes.
(d) Properties of grain boundaries in the electrolyte such as impurity segregation and space charge play an important role in the ionic conductivity, especially at low temperatures. Certain additives can be used to scavenge the grain boundaries to enhance the ionic conductivity. The high resistivities of high-purity grain boundaries have been explained on the basis of space charges and depletion of oxygen vacancies in the vicinity of grain boundaries. The space charge layer in the electrolyte is an intrinsic property and no effective routes to overcome this barrier and improve the electrical conductivity have been demonstrated.

(e) The existence of microdomains has been demonstrated to have a great influence on the ionic conductivity. Engineering of microdomains would provide a new approach for achieving enhancement in the ionic conductivity of solid electrolytes.

(f) Many researchers have revealed the dependence of electrical conductivity on grain size, particularly, the increase of specific grain boundary conductivity. However, this increase seems to be the increase of electronic conductivity instead of ionic conductivity. The brick-layer model has predicted a decrease in ionic conductivity and increase in electronic conductivity when decreasing grain size. There also exists a discrepancy regarding the data on grain size on the electrical conductivity. More direct measurements of the ionic conductivity are required to better understand the grain size influence on the ionic conductivity.

(g) Processing conditions also influence the final ionic conductivity depending on the specimen density, the level of impurities, thermal history, and the formation of microdomain.

(h) Further improvement of the ionic conductivity in the zirconia- or ceria-based electrolytes may be realised by introducing a liquid phase either in the grain boundaries or by forming composite electrolytes.

Acknowledgments

References

[1] U. Stimming, S.C. Singhal, H. Tagawa, W. Lehnert (Eds.), Proc. of SOFC-VIII, The Electrochem. Soc., 2002.

[2] V.V. Kharton, F.M.B. Marques, A. Atkinson, Solid State Ionics 174 (1–4) (2004) 135.

[3] T. Ishihara, J. Tabuchi, S. Ishikawa, J. Yan, M. Enoki, H. Matsumoto, Solid State Ionics 177 (2006) 1949.

[4] N.M. Sammes, G.A. Tompsett, H. Näfe, F. Aldinger, J. Eur. Ceram. Soc. 19 (10) (1999) 1801.

[5] N.Q. Minh Science, Technology of Ceramic Fuel Cells, Elsevier, Amsterdam, 1995.

[6] J.B. Goodenough, Annu. Rev. Mater. Res. 33 (2003) 91.

[7] H.L. Tuller, in: O.T. Sørensen (Ed.), Nonstiochiometric Oxides, Academic Press, New York, 1981.

[8] R.W. Vest, J.M. Honing, in: N.M. Tallan (Ed.), Electrical Conductivity in Ceramics and Glass, Marcel Dekker, New York, 1974.

[9] H. Inaba, H. Tagawa, Solid State Ionics 83 (1996) 1.

[10] M. Mogensen, N.M. Sammes, G.A. Tompsett, Solid State Ionics 129 (2000) 63.

[11] B.C.H. Steele, Solid State Ionics 129 (2000) 95.

[12] S.C. Singhal, K. Kendall (Eds.), High Temperature Solid Oxide Fuel Cells: Fundmentals, Design, and Applications, Elsevier Advanced Technology, Oxford, UK, 2003.

[13] K. Eguchi, T. Setoguchi, T. Inoue, H. Arai, Soild State Ionics 52 (1992) 165.

[14] H. Yoshida, H. Deguchi, K. Miura, M. Horiguchi, T. Inagaki, Solid State Ionics 140 (2001) 191.

[15] J.A. Kilner, in: R. Metselaar, H.J.M. Heijingers, J. Schoonman (Eds.), Solid State Chemistry, Elsevier Science Ltd., Amsterdam, 1982.

[16] D.J. Kim, J. Am. Ceram. Soc. 72 (1989) 1415.

[17] R.D. Shannon, Acta Crystallogr. A 32 (1976) 751.

[18] J.A. Kilner, R.J. Brook, Solid State Ionics 6 (1982) 237.

[19] C.R.A. Catlow, Solid State Ionics 12 (1984) 67.

[20] M.M. Bucko, J. Eur. Ceram. Sci. 24 (2004) 1305.

[21] J. Gong, Y. Li, Z. Tang, Z. Zhang, Mater. Lett. 46 (2000) 115.

[22] H. Kaneko, F. Jin, H. Taimatsu, H. Kusakabe, J. Am. Ceram. Soc. 76 (1993) 793.

[23] D.P.F. De Souza, A.L. Chinelatto, M.F. De Souza, J. Mater. Sci. 30 (1995) 4355.

[24] J.A. Kilner, Solid State Ionics 129 (1–4) (2000) 13.

[25] P. Wynblatt, G.S. Rohrer, F. Papillon, J. Eur. Ceram. Soc. 23 (2003) 2841.

[26] D.-S. Lee, W.S. Kim, S.H. Choi, J. Kim, H.-W. Lee, J.-H. Lee, Solid State Ionics 176 (2005) 33.

[27] Y. Shiratori, F. Tietz, H. Buchkremer, D. Stover, Solid State Ionics 164 (2003) 27.

[28] J.M. Ralph, J.A. Kilner, in: U. Stimming, S.C. Singhal, H. Tagawa, W. Lehnert (Eds.), Proc. of SOFC-V. The Electrochem. Soc. (1997) 1021.

[29] J.M. Ralph, J.A. Kilner, B.C.H. Steele, MRS Symp. Proc. 575 (2000) 309.

[30] D.L. Maricle, T.E. Swarr, S. Karavolis, Solid State Ionics 52 (1992) 173.

[31] T. Mori, J. Drennan, J. Lee, J. Li, T. Ikegami, Solid State Ionics 154/155 (2002) 461.

[32] T. Mori, T. Ikegami, H. Yamamura, J. Electrochem. Soc. 146 (1999) 4380.

[33] E.P. Butler, J. Drennan, J. Am. Ceram. Soc. 65 (1982) 474.

[34] J. Drennan, E.P. Butler, J. Am. Ceram. Soc. 65 (1982) C194.

[35] E.P. Butler, R.K. Slotwinski, N. Bonanos, J. Drennan, B.C.H. Steele, in: N. Claussen, M. Ruhle, A.T. Heuer (Eds.), Sci. and Tech. Of Zirconia II, Advances in Ceramics, vol. 12, Am. Ceramic. Soc., Columbus, OH (1984) 572.

[36] J. Drennan, E.P. Butler, in: P. Vincezini (Ed.), Science of Ceramics, vol. 12, Ceramurgica, Faenza, Italy, 1984.

[37] B.C.H. Steele, E.P. Butler, Proc. Br. Ceram. Soc. 36 (1985) 45.

[38] X. Guo, W. Sigle, J. Fleig, J. Maier, Solid State Ionics 154/155 (2002) 555.

[39] M. Miyayama, H. Yanagida, A. Asada, Am. Ceram. Soc. Bull. 64 (1985) 660.

[40] A.J. Feighery, J.T.S. Irvine, Solid State Ionics 121 (1999) 209.

[41] S.P.S. Badwal, J. Drennan, J. Aust. Ceram. Soc. 20 (1984) 28.

[42] T. Zhang, Z. Zeng, H. Huang, P. Hing, J. Kilner, Mater. Lett. 57 (2002) 124.

[43] Y. Mishima, H. Mitsuyasu, M. Ohtaki, K. Eguchi, J. Electrochem. Soc. 145 (3) (1998) 1004–1007.

[44] W.S. Jang, S.H. Hyun, S.G. Kim, J. Mater. Sci. 37 (12) (2002) 2535.

[45] T. Inoue, T. Setoguchi, K. Eguchi, H. Arai, Solid State Ionics 35 (3/4) (1989) 285.

[46] J.H. Lee, S.M. Yoon, B.K. Kim, H.W. Lee, H.S. Song, J. Mater. Sci. 37 (2002) 1165.

[47] T. Horita, N. Sakai, H. Yokokawa, M. Dokiya, T. Kawanda, J. Van Herle, K. Sasaki, J. Electroceramics 1 (2) (1997) 155.

[48] A. Tsoga, A. Naoumidis, D. Gupta, Stover, Mater. Sci. Forum 308–311 (1999) 794.

[49] X.D. Zhou, B. Scarfino, H.U. Anderson, Solid State Ionics 175 (2004) 19.

[50] M. Price, J. Dong, X. Gu, A. Scott, E. Speakman, A. Payzant, T.M Nenoff, J. Am. Ceram. Soc. 88 (7) (2005) 1812.

[51] T.H. Kimpton, J. Randle, Drennan, Solid State Ionics 149 (1/2) (2002) 89.

[52] B. Zhu, Solid State Ionics 119 (1–4) (1999) 305.

[53] S. Azad, O.A. Marina, C.M. Wang, L. Saraf, V. Shutthanandan, D.E. McCready, A. El-Azab, J.E. Jaffe, M.H. Engelhard, C.H.F. Peden, S. Thevuthasan, Appl. Phys. Lett. 86 (2005) 131906.

[54] H. Matzke, in: O.T. Sorensen, J.A.O. Kilner, B.C.H. Steele (Eds.), Non-stoichiometric Oxides, Academic Press, New York, 1981, p. 156.

[55] M. Aoki, Y.-M. Chiang, I. Kosacki, J.-R. Lee, H.L. Tuller, Y.J. Liu, J. Am. Ceram. Soc. 79 (1996) 1169.

　　　S. Hui et al. / Journal of Power Sources 172 (2007) 493–502

[56] H.L. Tuller, Solid State Ionics 131 (2000) 143.
[57] P. Mondal, A. Klein, W. Jaegermann, H. Hahn, Solid State Ionics 118 (1999) 311.
[58] T. Van Dijk, A.J. Burggaaf, Phys. Status Solidi A. 63 (1981) 229.
[59] J. Maier, Ber. Bunsen. Phys. Chem. 90 (1986) 26.
[60] J. Maier, Prog. Solid State Chem. 23 (1995) 171.
[61] X. Guo, J. Maier, J. Electrochem. Soc. 148 (2001) E121.
[62] X. Guo, W. Sigle, J. Maier, J. Electrochem. Soc. 149 (2002) J73.
[63] P. Heitjans, S. Indris, J. Phys: Condens. Matter 15 (2003) R1257.
[64] S.P.S. Badwal, Solid State Ionics 76 (1995) 67.
[65] S.P.S. Badwal, S. Rajendran, Solid State Ionics 70/71 (1994) 83.
[66] R. Rower, G. knoner, K. Reimann, H.E. Schaefer, U. Sodervall, Phys. Stat. Sol. B 239 (2003) R1.
[67] X. Guo, Comp. Mater. Sci. 20 (2001) 168.
[68] J.M. Ralph, J.A. Kilner, B.C.H. Steele, Mater. Res. Soc. Symp. Proc. 575 (2000) 309.
[69] X. Guo, Solid State Ionics 96 (1997) 247.
[70] X. Guo, Solid State Ionics 99 (1997) 137.
[71] Y. Lei, Y. Ito, N.D. Browning, J. Am. Ceram. Soc. 85 (2002) 2359.
[72] E.C. Dickey, X. Fan, S.J. Pennycook, J. Am. Ceram. Soc. 84 (2001) 1361.
[73] R. Gerhardt, A.S. Nowick, M.E. Mochel, I. Dumler, J. Am. Ceram. Soc. 69 (1986) 641.
[74] D.Y. Wang, A.S. Nowick, J. Solid State Chem. 35 (1980) 325.
[75] S. Hong, K. Mehla, A. Virkar, J. Electrochem. Soc. 145 (1998) 638.
[76] J. Maier, Solid State Ion. 175 (2004) 7.
[77] I. Kosacki, C.M. Rouleau, P.F. Becher, J. Bentley, D.H. Lowndes, Solid State Ionics 176 (2005) 1319.
[78] F.T. Ciacchi, S.P.S. Badwal, J. Drennan, J. Eur. Ceram. Soc. 7 (1991) 185.
[79] S.P.S. Badwal, J. Drennan, Mater. Forum 16 (1992) 237.
[80] G. Brunauer, H. Boysen, F. Frey, H. Ehrenberg, J. Phys. Condens. Matter 14 (2002) 135.
[81] P.R. Slater, J.T.S. Irvine, T. Ishihara, Y. Takita, Solid State Ionics 107 (1998) 319.
[82] J. Drennan, V. Zelizko, D. Hay, F.T. Ciacchi, S. Rajendran, S.P.S. Badwal, J. Mater. Chem. 7 (1997) 79.
[83] R.O'Hayre, Y.-I. Park, F.B. Prinz, Y. Saito, Solid oxide electrolyte with ion conductivity enhancement by dislocation, US Patent Application no. 10449709 filed on May 29, 2003.
[84] X. Guo, Prog. Mater. Sci. 51 (2006) 151.
[85] Q. Fu, W. Zhang, R. Peng, D. Peng, G. Meng, B. Zhu, Mater. Lett. 53 (2002) 186.
[86] J. Maier, Electrochem. Indust. Phys. Chem. 68 (2000) 395.
[87] J. Schoonman, Solid State Ionics 135 (2000) 5.
[88] T.Y. Tien, J. Appl. Phys. 35 (1964) 122.
[89] I. Kosacki, B. Gorman, H.U. Anderson, in: T.A. Ramanarayanam, et al. (Eds.), Ionic and Mixed Conductors, vol. III, Electrochemical Society, Pennington, NJ, 1998, p. 631.
[90] A. Tschope, R. Birringer, J. Electroceram. 7 (2001) 169.
[91] Y.M. Chiang, E.B. Lavik, I. Kosacki, T.L. Tuller, J.Y. Ying, J. Electroceram. 1 (1) (1997) 7.
[92] R. Maric, S. Seward, P.W. Faguy, M. Oljaca, Electrochem. Solid-State Lett. 6 (5) (2003) A91.
[93] A.I. Ioffe, M.V. Inozemtsev, A.S. Lipilin, M.V. Perfilev, S.V. Karpachov, Phys. Status Solidi A 30 (1975) 87.
[94] M.J. Verkerk, B.J. Middlehuis, A.J. burggraaf, Solid State Ionics 6 (1982) 159.
[95] S.P.S. Badwal, J. Drennan, J. Mater. Sci. 22 (1987) 3231.
[96] X.J. Chen, K.A. Khor, S.H. Chan, L.G. Yu, Mater. Sci. Eng. A335 (2002) 246.
[97] P. Heitjans, S. Indris, J. Phys. Condens. Matter 15 (2003) R1257.
[98] S. Ramasamy, B. Purniah, PINSA 67A (2001) 85.
[99] J.F. Baumard, P. Abelard, Adv. Ceram. 12 (1984) 555.
[100] M. Kleitz, C. Pescher, L. Dessemond, in: S.P.S. Badwal, M.J. Bannister, R.H.J. Hannink (Eds.), Science and Technology of Zirconia V, Technomic, Lancaster, PA, 1993, p. 593.
[101] L. Dessemond, J. Guindet, A. Hammou, M. Klerta, in: F. Grosz, P. Zegers, S.C. Singhal, O. Yamamoto (Eds.), Proceedings of the 2nd International Symposium on SOFCs, Brussels, Belgium (1991) 409.
[102] I.R. Gibson, G.P. Dransfield, J.T.S. Irvine, J. Mater. Sci. 33 (1998) 4297.
[103] J.E. Shelmilt, H.M. Williams, J. Mater. Sci. Lett. 18 (1999) 1735.
[104] M. Hirano, M. Inagaki, J. Am. Ceram. Sec. 83 (2000) 2619.
[105] T. Mori, Y. Wang, J. Drennan, G. auchterlonie, Solid State Ionics 175 (2004) 641.
[106] K. Yamahara, C.P. Jacobson, S.J. Visco, L.C.D. Jonghe, in: S.C. Singhal, M. Dokiya (Eds.), Proceedings of the 8th International Symposium on SOFCs, Paris, France (2003) 187.